

## Crystalline Transfer RNA: The Three-Dimensional Patterson Function at 12-Angstrom Resolution

**Abstract.** *An orthorhombic form of crystalline formylmethionine transfer RNA has been obtained which contains one molecule as the asymmetric unit of the unit cell. Three-dimensional x-ray diffraction data have been collected up to a resolution of 12 angstroms, and from this a Patterson function has been calculated. The function contains an elongated ridge of interatomic vectors parallel to the c-axis of the crystal. Analysis of the function suggests that the molecules are elongated and dimerized in an overlapping antiparallel fashion along the c-axis. The dimer has a length near 109 angstroms and a width of 35 angstroms in one direction. The individual molecular length is approximately 80 angstroms with an irregular cross section measuring 25 by 35 angstroms.*

Transfer RNA (tRNA) is of great importance in the molecular biology of living systems. This molecule can be activated by specific enzymes so that an amino acid is attached to one end. In its activated form tRNA enters the ribosome where it interacts with messenger RNA and participates in the formation of a polypeptide chain during protein synthesis. The molecule thus has a highly specific role in the translation of information from the nucleic acids into the proteins in biological systems. Because of this central role in the expression of genetic information, there is considerable interest in understanding the three-dimensional configuration of the molecule and the manner in which it carries out its biological functions. Transfer RNA's have 75 to 85 nucleotides, and the primary sequence of more than a dozen purified species has now been determined (1). This has led to a generally accepted cloverleaf model in which the polynucleotide strand folds back on itself to form short, looped, double-helical portions held together by hydrogen bonding between the purine and pyrimidine bases. If this secondary structure is correct, it is important to understand the manner in which these folded regions are packed together to form the actual three-dimensional structure of the molecule.

The crystallization of a macromolecule is a significant step in determining its molecular structure. Crystalline proteins have been studied for a long time, and during the past few years structures of several proteins have been solved by x-ray diffraction. The recent crystallization (2-5) of tRNA has raised the prospect that a similar program will ultimately lead to a detailed knowledge of its three-dimensional configuration. We have reported (3, 6) the formation of two different types of crystalline formylmethionine tRNA. Here we report the analysis of the

three-dimensional x-ray diffraction data collected up to a resolution of 12 Å from one of these crystal forms. Using this data, we have calculated a three-dimensional Patterson function. The crystal used has only one molecule of tRNA in the asymmetric unit, and we have been able to interpret this Patterson function to learn something about the shape and packing of the tRNA molecule in the crystalline state.

Our initial crystallization experiments were carried out with *Escherichia coli* formylmethionine tRNA in a water-chloroform system containing magnesium ions as the only divalent cation (3, 5). This yielded a heavily hydrated, crystalline hexagonal prism which produced an x-ray diffraction pattern with a resolution of only 20 Å (Table 1). However, by crystallizing this molecule from a solution of ethanol and water

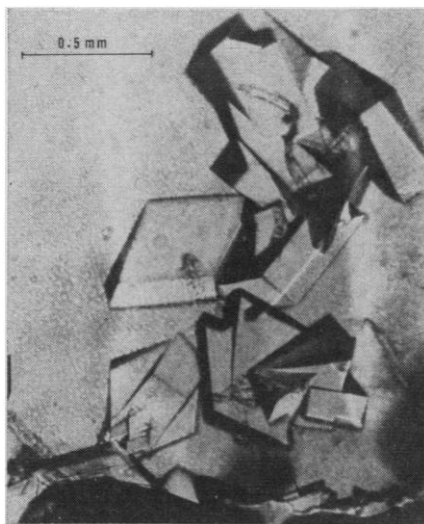


Fig. 1. Orthorhombic crystals of formylmethionine tRNA. The crystals were formed in an aqueous solution which had been equilibrated with 7 percent ethanol at 4°C. Concentration of materials used was as follows: 3.4 mg of tRNA per milliliter, 5 mM MgCl<sub>2</sub>, 5 mM tris(hydroxymethyl)aminomethane (pH 7.0), 5 mM KCl, and 1 mM MnCl<sub>2</sub>.

with a mixture of magnesium and manganese cations in a ratio of 5 to 1, large orthorhombic crystals were formed (Fig. 1) (6). These crystals have well-defined faces and produce an x-ray diffraction pattern with a limiting 7 Å resolution. Its characteristics are listed in Table 1. The hexagonal crystals have several molecules in an asymmetric unit while the orthorhombic crystals have only one molecule. The latter crystals also have a moderate degree of hydration (62 percent) comparable to many protein crystals (7). A sample oscillation diffraction pattern is shown in Fig. 2, where there is a full representation of the diffraction data out to a limit of 12 Å. Photographic data were collected at 4°C with an AMR micro-focus x-ray diffraction tube stand by both oscillation and precession techniques. The intensities were measured with a Joyce Loebel densitometer, and no absorption corrections were made. The 12-Å data from the orthorhombic form of the formylmethionine tRNA crystals contain a total of 61 reflections with a measurable intensity above background.

The Patterson function can be calculated directly from the x-ray intensity data without knowing the phases of the reflections. This function represents all the interatomic vectors in the unit cell of the crystal. If there is a high peak in the Patterson map, it means that there are many interatomic vectors with a length and direction equal to that from the origin to the peak. The water molecules in the crystal are largely disordered, and the major contribution to the diffracted intensity is due to the scattering by the tRNA molecules. The interatomic vectors are thus produced by the atoms of the tRNA molecule itself. In the case of tRNA, the concentration of electrons in the chain of phosphate groups along the backbone of the molecule is higher than other parts of the molecule. Because the phosphate groups are likely to be near the surface of the molecule, the contrast in scattering power between the tRNA and the aqueous environment may be somewhat greater than that found in analogous studies of hydrated crystalline proteins. In the early development of protein crystal analysis, low resolution Patterson functions were used to determine the size, shape, and packing of the protein molecules in the crystal.

The orthorhombic form of crystalline formylmethionine tRNA was selected for analysis because the unit cell

is relatively small and it has one molecule in an asymmetric unit. This is of great value because it may allow one to differentiate the intramolecular interatomic vectors, those arising from within one tRNA molecule, from the interatomic vectors arising between different molecules in the same unit cell. We might thus anticipate that the interatomic vectors from within one molecule would add together to form a continuum of vector density connected to the origin of the Patterson function. The number of contours in the Patterson map is related to the number of vectors in the section. Figure 3 shows six different sections of the three-dimensional Patterson function taken at intervals of  $1/20$  of the  $a$ -axis, that is, 3.16 Å. At the upper left-hand corner is the Patterson section at the 0 level of the  $a$ -axis. The function is plotted only out to a distance of  $c/2$  and  $b/2$  because, by Patterson symmetry for the space group  $C222$ , the remainder of the function can be generated by mirror planes, one perpendicular to the  $c$ -axis and the other perpendicular to the  $b$ -axis at values of  $c/2$  and  $b/2$ , respectively. Thus the function along the  $c$ -axis is plotted to a distance of 54.7 Å, and along the  $b$ -axis to 53.5 Å. Six sections are shown in Fig. 3 up to  $1/4$  the distance along the  $a$ -axis or 15.8 Å. At that distance there is a twofold axis of symmetry parallel to  $c$  and lo-

Table 1. Crystal forms of formylmethionine tRNA.

| Measurements                  | Hexagonal                               | Orthorhombic                                   |
|-------------------------------|---|--|
| Space group                   | $P6_3$ or $P6_322$                      | $C222$   |
| Cell parameters               | $a = 170$ Å<br>$b = 234$ Å              | $a = 63.2$ Å<br>$b = 106.9$ Å<br>$c = 109.3$ Å |
| Volume                        | $5.83 \times 10^6$ Å <sup>3</sup>       | $7.39 \times 10^5$ Å <sup>3</sup>              |
| Density                       | 1.12 g/cm <sup>3</sup>                  | 1.38 g/cm <sup>3</sup>                         |
| Molecules per asymmetric unit | 5 or 6 (if $P6_3$ )<br>3 (if $P6_322$ ) | 1  |
| Solvent % (volume)            | 87.5%                                   | 62%  |
| Highest resolution            | 20 Å                                    | 7 Å  |

ated at  $1/4$   $b$  so that the function repeats itself with inversion. The section at a value of  $6/20$   $a$  is thus the same as that shown at  $4/20$   $a$  except for the inversion of the top and bottom of the diagram, and so forth. The entire Patterson function is therefore represented in Fig. 3. Figure 4 shows the Patterson section at the 0 level along the  $b$ -axis. In both Figs. 3 and 4 the dashed line is the zero value of the Patterson function and the dotted areas represent negative regions.

There are two different types of vectors found in the Patterson function. One of these is self vectors—that is, vectors originating from and ending at the same atom. Each atom contributes a vector of this type, and they are all found at the origin of the Patterson function. This produces many contours

at the origin which are directly related to the number of atoms in the unit cell but are not related to the shape of the molecule. The accumulation of self vectors can be seen at the origin in both Figs. 3 and 4. The other Patterson vectors are those found between different atoms. As mentioned above, the interatomic vectors from within one molecule may often show up as an isolated region separated from those peaks which arise from the vectors between two atoms from two different molecules. This is usually the case unless two molecules are closely joined together. If we look at the 0 level section in Fig. 3 (upper left-hand corner), we see that, in addition to the accumulation of self vectors at the origin, there is a continuum in the vector function extending along the top of the diagram in the direction of the  $c$ -axis. This continuum is clearly separated by negative values from two other peaks which are below it. The continuum along the  $c$ -axis has a three-dimensional form and is well represented in three or four sections along the  $a$  axis. Another interesting feature of this ridge is a second bulge which starts at approximately 35 Å along the  $c$ -axis and extends from there to the end of the axis at  $c/2$ . This bulge can be clearly seen in the 0 level and  $1/20$  level section of Fig. 3, as well as in the 0 level section of Fig. 4. The continuous ridge of Patterson vectors parallel to the  $c$ -axis suggests that the molecule is elongated and lying in this direction. An estimate of the diameter of the tRNA is obtained by symmetry constraints. There are twofold axes which limit the width of the molecule in one direction to be less than 30 Å if the elongated molecule is lying along the  $c$ -axis.

An important class of intermolecular vectors are those between molecules which are related by twofold screw axes. The space group  $C222$  has twofold screw axes along the  $a$  and  $b$  axes. These generate special peaks which occur in the Patterson sections at  $x = a/2$  (equivalent to Fig. 3, upper left, with top and bottom inverted), and in the Patterson at  $y = b/2$  (equivalent to Fig. 4, with top and bottom inverted). We have identified the two special peaks which allow us to locate the centers of the molecules in the unit cell (8). The elongated molecules are paired together with their centers displaced along the  $c$ -axis by 45 Å and along the  $a$ -axis by approximately 5 Å. The two elongated molecules in the dimer are antiparallel to each other with a considerable over-

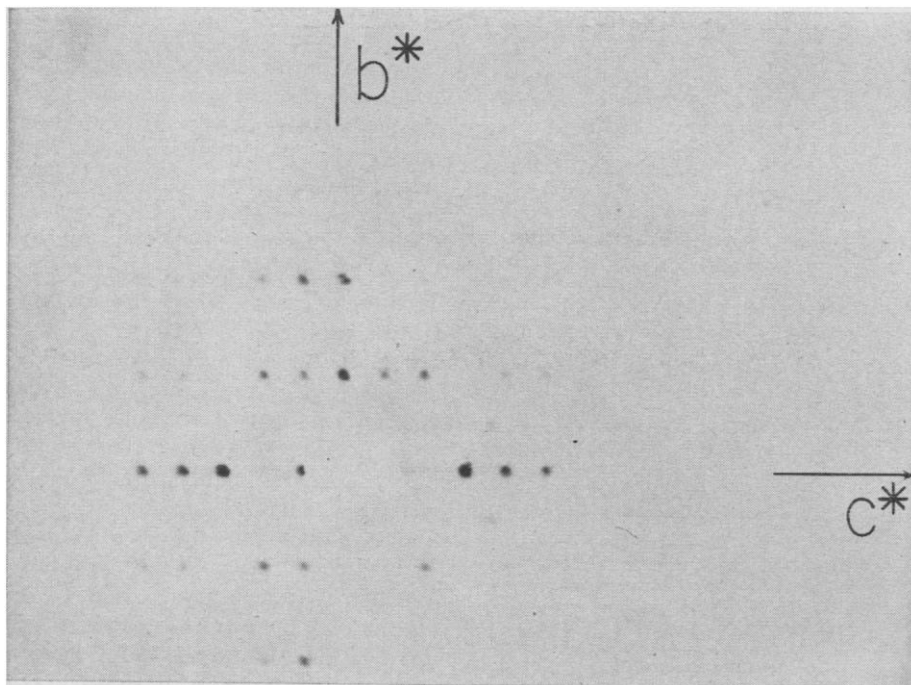


Fig. 2. An oscillation photograph showing the x-ray diffraction pattern of orthorhombic formylmethionine tRNA crystals. The crystal mounted in a sealed quartz capillary with mother liquor was oscillated approximately  $\pm 15^\circ$  around the  $b$ -axis at a distance of 10 cm from the crystal to the film. Reflections appear both from the  $0kl$  and  $1kl$  layers.

lap along their length. The length of the dimer pair should be close to the length of the  $c$ -axis, 109 Å. The separation between the molecules is approximately 35 Å along the  $b$ -axis. This gives rise to the large peak found in the zero level Patterson section (Fig. 3) at the center left. It is interesting to note that the dimerization leads to a packing in the unit cell which is very close to hexagonal, even though the crystal is orthorhombic. This suggests that dimer assembly may also be involved in the formation of the more complex hexagonal lattice found for formylmethionine tRNA (Table 1).

Since the dimerization of tRNA has also been reported in solution studies (9), it is possible that the phenomenon is general and will be found in many crystal lattices.

It is somewhat more difficult to obtain a reliable figure for the length of the individual molecule. Using the information available concerning the separation of the molecular centers of the dimer along the  $c$ -axis, we can make a rough estimate of the molecular length of approximately  $80 \pm 10$  Å. At the present time we are not certain of the extent of the overlap region in the dimer.

Other features of the Patterson function are worth noting. The continuous ridge of Patterson vectors parallel to the  $c$ -axis is not smooth. In sections  $3/20$  to  $5/20$   $a$ , it can be seen that this ridge has some lumps on it, some of which are also visible in the Patterson section shown in Fig. 4. These mean that the molecule is not rounded in cross section but has some irregular features which are recognizable even at the comparatively low resolution of 12 Å. We have also calculated a three-dimensional, sharpened Patterson function which sharpens many of the features. The general quality of the Patterson function remains unchanged although more details are visible. However, in view of the fact that the Patterson function was calculated with only limited data at 12-Å resolution, we do not wish to draw further interpretations until additional data are accumulated.

We have carried out another calculation which reinforces our interpretation that the RNA molecule is lying along the  $c$ -axis of the crystal. In this elongated form, it is likely that the molecule does not have the double-helical arms of the cloverleaf model of tRNA extending out in different directions. Instead it is likely that they are folded together in a fairly compact form so that the axes of the double helices may lie generally along the axis of the molecule. We have tested this assumption by calculating a comparison of the diffraction intensity which would be produced by a double-helical fragment of RNA containing five base pairs (as seen in the cloverleaf model) and that observed by the crystalline formylmethionine tRNA. A search function was used to compare the calculated with the observed data as a function of various orientation angles (10). The results of these calculations indicate that the best fit is found when the small double helical RNA fragments are ori-

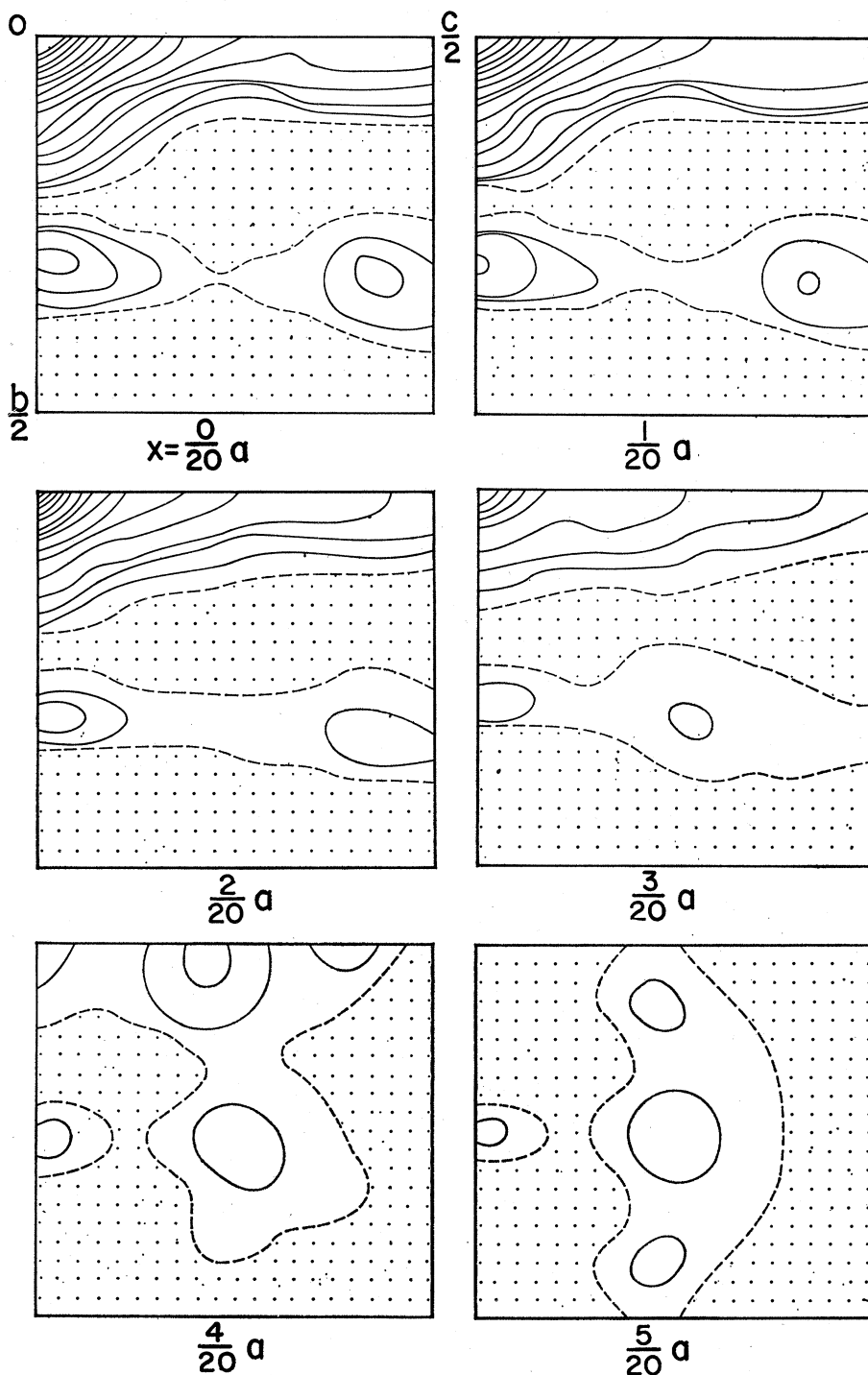


Fig. 3. A three-dimensional Patterson function of crystalline formylmethionine tRNA. The function is plotted out to values of  $b/2$  (53.5 Å) and  $c/2$  (54.7 Å). The Patterson function has mirror planes perpendicular to the  $c$ -axis and the  $b$ -axis at  $c/2$  and  $b/2$ ; therefore only  $1/4$  of the Patterson function is illustrated at each level. A twofold rotation axis occurs parallel to the  $c$ -axis at a distance a quarter of the way along  $a$ . The function thus repeats itself as one continues further up the  $a$ -axis. The  $6/20$   $a$  section is the same as  $4/20$   $a$  with top to bottom inversion, and so forth. The dashed lines are the zero level of the Patterson function while the dotted areas are negative regions.

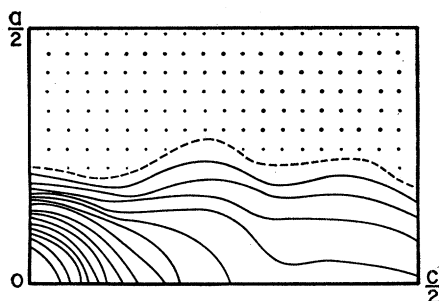


Fig. 4. Patterson section along the zero level of the  $b$ -axis. In addition to the maximum at the origin there are two other bulges in the function.

ented roughly parallel to the  $c$ -axis. These calculations thus reinforce the interpretation of the Patterson calculation which indicates that the molecule lies parallel to the  $c$ -axis.

A three-dimensional Patterson calculation is an intermediate stage in the crystallographic analysis of tRNA. At 12-Å resolution it is clear that we are unable to proceed very far in interpreting the detailed folding of the molecule. However, with a favorable unit cell, the Patterson function at this resolution is able to depict some of the gross features of the molecule and indicates the manner in which they are packed together in the unit cell. Analysis of the 12-Å data has led us to the conclusion that the molecule has an elongated form and is dimerized in an antiparallel fashion with partial overlapping along the length of the molecule. The length of the dimer is about 109 Å. An individual molecule has a length of  $80 \pm 10$  Å and a width near 25 Å in one

direction and 35 Å in another direction. The molecule is thus not rounded in cross section but has irregular features, the detailed nature of which will have to await the result of a higher resolution x-ray diffraction analysis.

SUNG-HOU KIM  
ALEXANDER RICH

Department of Biology,  
Massachusetts Institute of Technology,  
Cambridge 02139

#### References and Notes

1. See review by G. R. Phillips, *Nature* **223**, 374 (1969).
2. B. F. C. Clark, B. P. Doctor, K. C. Holmes, A. Klug, K. A. Marcker, S. J. Morris, H. H. Paradies, *ibid.* **219**, 1222 (1968); F. Cramer, F. v. d. Haar, W. Saenger, E. Schlimme, *Angew. Chem. Int. Ed. Engl.* **7**, 895 (1968).
3. S.-H. Kim and A. Rich, *Science* **162**, 1381 (1968).
4. A. Hampel, M. Labanauskas, P. G. Connors, L. Kirkegaard, U. L. Rajbhandary, P. B. Sigler, R. Bock, *ibid.*, p. 1384; J. R. Fresco, R. D. Blake, R. Langridge, *Nature* **220**, 1285 (1968).
5. B. S. Vold, *Biochem. Biophys. Res. Commun.* **35**, 222 (1969).
6. S.-H. Kim, P. Schofield, A. Rich, *Cold Spring Harbor Symp. Quant. Biol.* **34** (1969).
7. B. W. Matthews, *J. Mol. Biol.* **33**, 491 (1968).
8. The detailed crystallographic interpretation will be published elsewhere (S.-H. Kim and A. Rich, in preparation).
9. H. G. Zachau, *Eur. J. Biochem.* **5**, 559 (1968).
10. M. Zwick, thesis, Massachusetts Institute of Technology (1968); J. Sussman, personal communication.
11. We thank Dr. P. Schofield for setting up the crystallization method for the orthorhombic form of formylmethionine transfer RNA, J. Sussman for computational assistance in the helix search calculation, and Dr. F. Bergmann of the National Institute of General Medical Sciences and Dr. G. D. Novelli of the Oak Ridge National Laboratories for advice and assistance in obtaining the samples of purified tRNA. The material was produced at the Oak Ridge National Laboratories under an inter-agency contract with the U.S. Atomic Energy Commission and the NIGMS. Supported by grants from the NIH, NSF, and NASA, the National Science Foundation and the National Aeronautics and Space Administration.

22 October 1969

## Mouse Leukemia Virus Activation by Chemical Carcinogens

**Abstract.** *The induction of lymphomas in C57BL mice by methylcholanthrene, urethan, or diethylnitrosamine was accompanied by the development of murine leukemia viral antigen in most of the lymphoid tumors. The cell-free transmission of lymphomas induced by methylcholanthrene and the development of antibody to murine leukemia virus prior to the detection of overt lymphoma in these mice suggest that unmasking of a latent leukemia virus is an indigenous acting cause of the lymphomas.*

Many chemical carcinogens have been studied in mice, but the mechanism of neoplastic transformation by these chemicals remains unclear. Intermediary events preceding transformation seem likely because of the multiplicity of cellular and humoral effects of chemical carcinogens in vivo. Several investigators who recovered leukemogenic agents from tumors induced by chemicals, including methylcholanthrene (1), urethan (2), and 7,12-dimethyl-

benz(a)anthracene (3), have suggested that activation of a latent oncogenic virus may play a role in chemical carcinogenesis. These studies were based on the demonstration of leukemogenic activity of very limited numbers of cell-free preparations, and thus the frequency and significance of finding leukemogenic virus in chemically induced lymphomas is subject to question.

The activation of a latent leukemogenic virus and induction of lym-

phoma in C57BL mice by radiation is well documented. Leukemogenic activity of cell-free filtrates from lymphomas induced by radiation in C57BL mice has been shown (4) and confirmed (5). The presence of a latent leukemia virus in the C57BL strain, which has a relatively low incidence of spontaneous leukemia, provides a model system for the study of chemically induced lymphomas.

During several long-term experiments on virus-chemical cocarcinogenesis with C57BL mice, we found that murine leukemia virus (MuLV) complement-fixing antigen (6) was present in a significant proportion of chemically induced lymphomas. This report concerns the relation between the development of lymphoid tumors and the induction of MuLV antigen in the lymphomatous tissues of chemically treated mice.

Test groups of 60 to 75 newborn C57BL/6 mice (Cumberland View Farms, Clinton, Tennessee) were housed in disposable plastic cages with filter-top lids and fed a standard mouse diet, with the addition of apples. Crystalline 3-methylcholanthrene (7) was dissolved in trioctanoin vehicle at concentrations of 10 and 100  $\mu\text{g}$  per 0.05 ml. One group of mice less than 24 hours old received 10  $\mu\text{g}$  of methylcholanthrene intraperitoneally, and another group received 100  $\mu\text{g}$ . In other experiments urethan (7) was dissolved in Hanks' basal salt solution. One group was given 5 mg of urethan subcutaneously when the animals were 7 and 9 days old. Another group was given 0.5 mg of urethan per gram of body weight weekly for 10 weeks beginning 1 week after birth. Diethylnitrosamine (7) was diluted in Hanks' basal salt solution at concentrations of 1, 4, 16, and 64  $\mu\text{g}$  per 0.05 ml. One group of 1-day-old mice was inoculated intraperitoneally with each of the four concentrations of diethylnitrosamine. Control groups included 1-day-old mice inoculated intraperitoneally with 0.05 ml trioctanoin, mice inoculated subcutaneously with 0.05 ml of Hanks' basal salt solution on days 7 and 9, and mice inoculated subcutaneously with 0.05 ml of Hanks' basal salt solution on day 1. All mice were weaned and separated by sex at 3 weeks of age; they were palpated twice weekly for detection of tumors or enlarged lymph nodes. Lymphomatous mice were killed, and clarified 10 percent extracts of various tissues were screened at a 1:2 dilution for the presence of complement-fixing antigen against rat antiserum group reac-